Critical Reviews™ in Biomedical Engineering, 47(3):235–247 (2019)

Electrochemical Detection of Fertility Hormones

Mukund Khanwalker,[a] Jared Johns,[a] Mackenzie M. Honikel,[a] Victoria Smith,[a] Stephanie Maxwell,[a] Sandhya Santhanaraman,[a] & Jeffrey La Belle[a,b,*]

[a]School of Biological and Health Systems Engineering, Arizona State University, Tempe, AZ; [b]Biodesign Institute at Arizona State University, Tempe, AZ

*Address all correspondence to: Dr. Jeffrey La Belle, School of Biological and Health Systems Engineering 501 E. Tyler Mall St. Tempe, AZ 85287; Tel.: 480-727-9061, E-mail: Jeffrey.Labelle@asu.edu

ABSTRACT: Fertility hormone levels are constantly changing, but it is crucial for a woman to be able to monitor her fertility levels if she is interested in conceiving. Women and physicians often have a difficult time determining ovulation windows due to fluctuating menstrual cycles and inaccurate interpretations of hormone levels. Current methods of fertility monitoring include physical or vaginal exams, laparoscopy, ultrasound scans, as well as evaluation of hormone levels. A rapid, at-home fertility monitoring tool can help alleviate the apprehensiveness associated with routine screenings and give women the privacy desired when trying to conceive. Herein, we discuss the development of an electrochemical biosensor for quantification of three fertility hormones: beta-estradiol, progesterone, and FSH. Each biomarker's MRE was immobilized onto a gold disk electrode through the use of self-assembled monolayer linking chemistry. Using electrochemical impedance spectroscopy (EIS), the biomarker concentration was correlated to impedance magnitude. An optimal binding frequency was identified for each biomarker, permitting simplistic hardware requirements and investigation into multimarker detection. Analytes were tested in both purified solutions and 1%–90% whole blood. Each biomarker exhibited a unique imaginary impedance peak and optimal binding frequency. The determination was made by assessing the response parameters including the linear fit correlation across the physiological hormone ranges. The existence of unique optimal frequencies permits for simultaneous detection of multiple hormones in a single test. Additionally, the identified frequency was robust across purified and complex solutions. Response characteristics were negatively impacted by the introduction of blood-based contaminants. However, the introduction of Nafion membranes, similar to ones used in commercial glucose sensors, is both feasible and beneficial.

KEY WORDS: electrochemical impedance spectroscopy, fertility, hormone detection

ABBREVIATIONS: 16-MHDA, 16-mercaptohexadecanoic; **CV**, cyclic voltammetry; **E3G**, oestrone-3-glucuronide; **EDC**, 1-ethyl-3-[3-dimethylaminopropyl] carbodiimide hydrochloride; **EIS**, electrochemical impedance spectroscopy; **ELISA**, enzyme linked immunosorbent assays; **Ferro**, potassium hexacyanoferrate (II) trihydrate; **Ferri**, potassium hexacyanoferrate (III); **FSH**, follicle stimulating hormone; **GDE**, gold disk electrode; **HSG**, hysterosalpingography; **HyCoSy**, hystero-contrast sonography; **LH**, luteinizing hormone; **LLD**, lower limits of detection; **MRE**, molecular recognition element; **NHS**, *N*-hydroxysulfosuccinimide; **OBF**, optimal binding frequency; **PBS**, phosphate buffered saline; **POC**, point-of-care; **Redox**, reduction-oxidation; **SAM**, self-assembled monolayer; **SIS**, saline infusion sonohysterosalpingography

I. INTRODUCTION

More than 3 million couples in the United States struggle with infertility, with 40% of these cases being attributed to women.[1] From 2006 to 2010, 12% of women in their child-bearing years sought some form of medical help to become pregnant or to prevent a miscarriage.[2] Several factors are associated with infertility. Some of these factors include patient age, the cervical factor, the tubal factor, and the peritoneal factor.

Increasing patient age can lead to decreasing quantity and quality of reproductive cells called oocytes, resulting in the decrease of sperm–egg fusion.[1,3] The cervical environment can cause infertility through chemical and physical properties of the cervical mucus.[3] These properties can lead to reduced sperm penetration.[4] Tubal factor infertility can occur when damaged fallopian tubes inhibit the transport of female reproductive cells in the opposite direction of sperm cells.[5] The phenomenon reduces the chances of pregnancy. Infertility associated with the peritoneal factor is related to pelvic adhesions that lead to obstruction of fallopian tubes and further block the mobility of oocytes.[6]

One of the main reasons couples have difficulty conceiving is their inability to accurately predict the

0278-940X/19/$35.00

female's ovulation period. Ovulation is a response to different hormone concentrations in the blood and occurs at regular intervals. However, these intervals are different for every woman.[7] Mapping out the concentrations of the central hormones related to inducing ovulation can produce an accurate timeline of an individual woman's menstrual and ovulatory cycle, which could help identify the optimum time to conceive. These key hormones include follicle stimulating hormone (FSH), estradiol, progesterone, and luteinizing hormone (LH).

A. Relevant Hormones

1. Follicle Stimulating Hormone

Follicle stimulating hormone is a glycoprotein produced in the pituitary gland that targets the granulocyte cells of the ovary in women.[8] FSH stimulates follicle growth and maturation in maturation in the ovary, inducing many potential follicles to develop. As FSH levels rise, a dominant follicle will emerge, from which the egg will burst during ovulation.[9,10] However, FSH levels decline before such an event can occur, requiring LH for the final step in ovulation.[10] FSH also stimulates the production of additional hormones, working alongside LH to regulate ovulation and preparation for fertilization and pregnancy.[9] As FSH concentration decreases with age and other factors, follicle quantity and quality declines, resulting in diminished ovarian reserve.[11] Elevated FSH levels (> 9iU/L) can also indicate infertility as the body indicates to the brain that the ovarian reserve needs more FSH to stimulate follicle growth.[12,13] Such a direct link between fertility and FSH makes it a standard target hormone for many hormone-based fertility tests.[11]

2. Luteinizing Hormone

Like FSH, luteinizing hormone (LH) is a glycoprotein produced in the pituitary gland that stimulates follicle growth, playing an integral role in ovulation.[9,10,14] Both LH and FSH hormones together stimulate normal follicular growth.[15] LH levels are generally low until a dominant follicle has emerged, at which point FSH concentration declines and LH levels spike, prompting the follicle to rupture and trigger ovulation.[10,16] LH also serves as a regulator for additional hormones, namely estradiol and progesterone, to prepare the body for pregnancy, as discussed below.[14]

3. Progesterone

Progesterone is a steroid produced by the corpus luteum, a hormone-producing structure in the ovary formed at the follicle after ovulation.[14] The secretion of progesterone occurs in the later stages of ovulation and is responsible for the thickening and maintenance of the endometrium (uterine wall).[17] This is essential for embedding and nourishing a fertilized embryo in the endometrium and, thus, is essential for a successful pregnancy. If fertilization does not occur, the corpus luteum disintegrates and progesterone production ceases, causing endometrial tissue to disperse as menstruation.[17] If fertilization does occur, progesterone production continues and is secreted by the placenta during the seventh week of pregnancy. Progesterone concentration, which is heightened specifically during ovulation, provides a reliable method of fertility testing.[18]

4. Estradiol

Estradiol is the main form of estrogen in the body. Like progesterone, estradiol is also secreted by the corpus luteum; it stimulates endometrial thickening in preparation for fertilization.[14,19] Estradiol concentrations are dependent on fertilization, and they decrease when the corpus luteum disintegrates. An estradiol surge, significant hormonal increase, is a precursor to the peak phase of ovulation. By detecting the rise in concentration of estradiol, which changes from 10 to 500 pg/mL of blood, the peak and window of ovulation can accurately be predicted and recorded.[20]

B. Current Methods of Detections

Clinicians use several imaging techniques to determine whether a woman is capable of conceiving: hysterosalpingography (HSG), laparoscopy, saline infusion sonohysterosalpingography (SIS), and hysterocontrast sonography (HyCoSy).[21] Each of these ap-

proaches are accurate in determining fertility. Fertility determination is accomplished through the assessment of fallopian tubes, which are essential for the transport of gametes and embryo.[21] The imaging techniques, however, are characteristically invasive, which can cause pain and discomfort for the patient. Ultrasound imaging can be used as an alternative method; it is noninvasive. The drawback of ultrasound is that it can only be used as a diagnostic tool to analyze the uterus.

The biosensor industry has been dominated by optics-based sensors, with many of its applications being used in the medical field. Optical biosensors are categorized into labeled and label-free methods. The most commonly used labeled method is enzyme-linked immunosorbent assays (ELISA), which tracks the target analyte via a fluorescent dye with high sensitivity.[22,23] The procedure and preparation of necessary antigens, however, can be prolonged and complicated, which can lead to varying forms of human error during measurement of the analyte or substance. Current fertility monitors use the principles of ELISA and optical biosensors through a disposable dual assay test stick that detects LH and oestrone-3-glucuronide (E3G).[24] LH levels are measured using a sandwich assay, in which the intensity of a line on the monitor increases as a concentration of LH in urine increases.[25] E3G levels are measured through a competitive assay, where line intensity decreases as the concentration of E3G increases.[25] E3G can provide an accurate picture of fertility levels and ovulation peaks. The disadvantage of such immunoassays is that they do not produce quantitative results or precise measurements of necessary hormones.

Label-free methods are more advantageous compared to labeled methods, due to a reduction in cost, time, and complexity.[26] We propose that electrochemical impedance spectroscopy (EIS) can be used to develop a simple, label-free biosensor capable of monitoring fertility levels and predicting ovulation peaks. Furthermore, a point-of-care (POC) device applying EIS would be able to quantify specific proteins or hormone concentrations. Hormones related to fertility, such as estradiol and FSH, are extremely low; they occur in concentration ranges of picograms per milliliter of blood. Progesterone is present in concentration ranges of nanograms per milliliter of blood. For such small concentrations, EIS has the high sensitivity required to accurately determine concentrations.[27] Such techniques have been successfully applied to other biomarkers like the detection of 1,5-anhydroglucitol, which is present in low concentrations when glucose levels are elevated.[28]

Hormones detected through EIS possess a specific optimal binding frequency (OBF). The OBF is the response that best represents ideal binding between hormones and their respective receptors or molecular recognition elements (MRE).[29] In the present study, β-estradiol, progesterone, and FSH were characterized using EIS, with the identification of OBFs for each hormone. By monitoring all three of these biomarkers, a woman can begin to create a picture of where her optimal fertility window is, as well as the potential hormone deficiencies causing her unsuccessful attempts at pregnancy.

II. MATERIALS AND METHODS

A. Chemicals and Reagents

The following chemicals were purchased from Sigma or Sigma-Aldrich (St Louis, MO, USA): 16-mercaptohexadecanoic (16-MHDA), 1-ethyl-3-[3-dimethylaminopropyl] carbodiimide hydrochloride (EDC), β-estradiol, progesterone, albumin, ethyl alcohol, ethanolamine, potassium hexacyanoferrate (II) trihydrate (Ferro), potassium hexacyanoferrate (III) (Ferri), potassium chloride. *N*-hydroxy–sulfosuccinimide (NHS) was purchased from Toronto Research Chemicals Inc. (Toronto, Ontario, Canada), and anti-17β-Estradiol antibody was obtained from Pierce Biotechnology (Rockford, IL, USA). Phosphate buffered saline (PBS) tablets were acquired from BioVision (Milpitas, CA, USA), and FSH was purchased from R&D Systems (Minneapolis, MN, USA). White New Zealand female rabbit whole blood was purchased from Bioreclamation (Westbury, NY).

B. Sample Preparation

The concentration gradient of estradiol covered a range of concentrations from 1 pg/mL to 500 pg/

mL, which spans the physiological range of estradiol for women during the menstrual cycle. All solutions of estradiol were frozen and stored in the −70°C freezer. Progesterone solutions were created via a serial dilution method, and PBS and ranged from 0.1 ng/mL to 100 ng/mL to cover the physiological range of progesterone. The same serial dilution method was used to create a concentration gradient for FSH ranging from 0.1 pg/mL to 10,000 pg/mL.

Electrochemical cells were created using a reduction-oxidation (redox) solution. In all experiments, the redox solution consisted of a 1:1 mixture of 5 mM potassium hexacyanoferrate (II) trihydrate and 5 mM of potassium hexacyanoferrate (III). For every experiment under pure conditions, 90 μL of redox solution was used with 10 μL of either PBS or a concentration of a hormone.

For nontarget experiments, concentrations of FSH (5–500 pg/mL), albumin (0.1–10 mg/mL), and progesterone (0.05–25 ng/mL) were made and combined with redox probe in the same ratio stated above. All concentrations were selected to fit within physiological ranges.

For experiments with blood, solutions of whole blood mixed with PBS were created to make concentrations of 1%, 10%, 25%, and 90% blood. These solutions were spiked with the same concentration ranges of FSH tested in pure conditions. Blood experiments were also performed on progesterone concentrations, using solutions of 5%, 10%, and 90% blood. The concentration gradient for progesterone was based on ranges tested in pure conditions as well.

C. Electrode Preparation and Antibody Immobilization

The immobilization schematic can be seen in Fig. 1. Gold-disk working electrodes, platinum counter electrodes, and Ag/AgCl reference electrodes were purchased from CH Instruments (Austin, TX). For each antibody test, each gold disk electrode (GDE) was polished using Buehler felt pads with 0.3 and 0.05 grit aluminum oxide. Each GDE was polished by tracing a figure-eight 150 times on each pad. After polishing and rinsing off the aluminum oxide from the surface, the electrodes were sonicated in deionized water (DI) for 20 minutes. The DI water was then replaced and sonicated for an additional 10 minutes. After sonication, the self-assembled monolayer (SAM) was generated through incubation of 1 mM 16-MHDA on the electrode surface. The activation of carboxylate groups was accomplished through a solution of 10 mM EDC and 40 mM NHS. An antibody solution (anti-FSH, antiprogesterone, or antiestradiol) of 100 μL was incubated on the electrode for 1 hour. A blocker via 1% ethanolamine was used to block all other active sites. The process was adapted from a published immobilization process.[30]

D. Electrochemical Equipment and Testing

All electrochemical measurements were conducted using a CHI660C Electrochemical Workstation or CHI Model 6005d Electrochemical Analyzer (CH Instruments, Austin, Texas). A cyclic voltammetry (CV) test is used to study the electrochemical properties of an analyte in a redox solution. A CV is run after sonicating the electrodes and is used to determine the formal potential of the sensor. It is achieved by sweeping +1.0 to −1.0 volts on clean electrodes. A plot of the oxidation and reduction peaks for the given redox solution is produced. By averaging the oxidation and reduction peak values the formal potential, or the DC offset of the electrochemical cell, is determined. On average, formal potential was found to be 150 mV across the tested electrodes.

After the respective antibody was immobilized onto the surface of the electrode, AC impedance testing was performed to determine the change in impedance with each addition of a higher concentration to the electrode system. In an AC impedance test, a sine wave was swept across a range of frequencies (0.1 Hz–100 kHz) at the formal potential determined for each electrode. All EIS tests performed on GDEs used the electrochemical cell setup previously explained.

In the nontarget experiments, the anti-FSH antibody was immobilized onto the electrode. However, instead of running a concentration gradient of FSH, concentration gradients of different hormones (nontargets) were used. The nontargets used in these

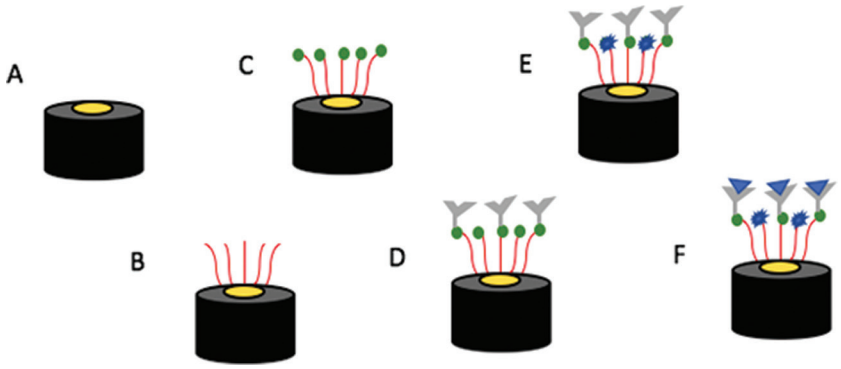

FIG. 1: (A) Bare polished gold surface, (B) assembly of SAM, (C) 10 mM EDC and 40 mM NHS (EDC/NHS), (D) immobilization of antibody, (E) ethanolamine blocker, (F) hormone binding to antibody

tests included progesterone, albumin, and estradiol. Progesterone and estradiol were chosen, as they are relevant fertility hormones tested within the study. Albumin was chosen due to its high concentration in blood, making it a potential interferent.

E. Determining OBF and Lower Limit of Detection

Impedance values were used to calculate slope [Ohm/Ln (concentration)] and goodness of fit (RSQ) for both linear and logarithmic concentrations at each frequency. For each hormone, OBF values were identified through location of peak slopes. RSQ values were demonstrated to be ≥ 0.8. The lower limit of detection (LLD) for each immobilized sensor was calculated using the equation: 3.3× standard deviation of blanks/slope.[31]

III. RESULTS AND DISCUSSION

A. Impedance Modes

Electrochemical impedance spectroscopy produces three different modes of impedance: complex (Z), real (Z′), and imaginary (Z″). As displayed in Fig. 2, a Nyquist plot is generated by plotting imaginary impedance versus real impedance. The imaginary impedance readings, which are associated with capacitance, are used to calculate peak slopes and OBFs.[32] Figure 2 also demonstrates how the magnitude of imaginary impedance values increases during each stage. The imaginary impedance values for the bare electrode ranges from 0 to a magnitude of 40 Ohms. The impedance values after the assembly of SAM and after immobilization of MRE, peaks at about a magnitude of 1600 Ohms and 10,000 Ohms, respectively.

B. Characterization of Hormones

Imaginary impedance overlays of each concentration were generated for each respective marker: estradiol, progesterone, and FSH. From the impedance plots (Fig. 3), imaginary impedance increases in magnitude as concentration is increased. Furthermore, there is an increase in capacitance as hormone levels are elevated. The OBF values correspond with the peak frequencies represented in Fig. 3. When studying Fig. 3A–C, a shift is clearly present in the OBFs for the target hormones. The OBFs for FSH, progesterone, and estradiol were 175.8, 8.071, and 1.74 Hz, respectively.

The observed shift could correlate with varying molecular weights for the antibody-antigen complex, with an increase in molecular weight resulting in higher OBFs. This finding demonstrated by the molecular weights of the antibody-antigen combination for FSH and progesterone; they are higher than the molecular weight of antibody-antigen combination of estradiol.

At the OBF (Fig. 4), the sensor demonstrated detection in the physiological domain. Detection in the physiological ranges is characterized by good

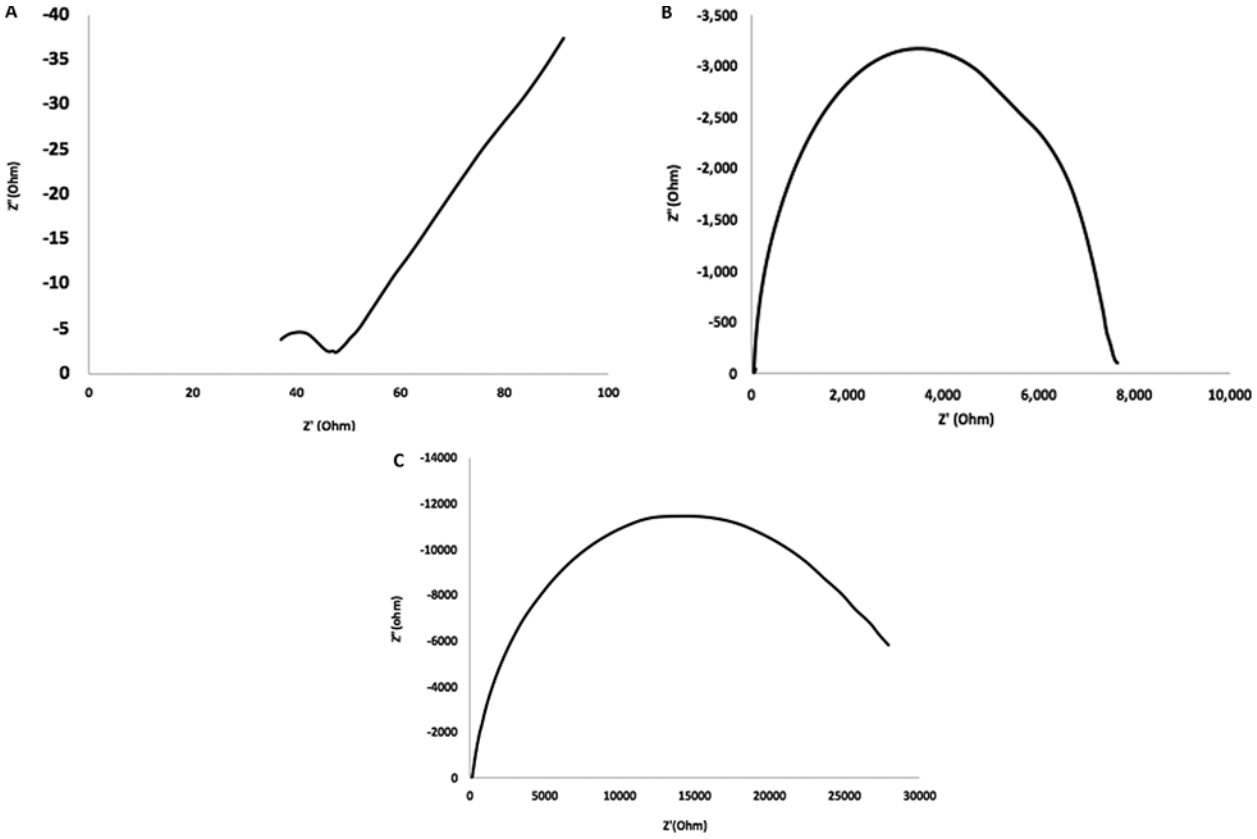

FIG. 2: (A) Nyquist of bare-polished GDE. (B) Nyquist after assembly of SAM. (C) Nyquist after immobilization of MRE or antibody

response and corresponding fit. The following finding is demonstrated through the calibration curves (Fig. 5), which are generated at the respective OBFs for each hormone. The LLDs for progesterone, estradiol, and FSH were 8.22 ng/mL, 2.35 pg/mL, and 4.02 pg/mL, respectively. A summary can be found in Table 1. These detection limits are superior to the current measurement standards of the three hormones.[33] The facts that each hormone has a different OBF and that each sensor is capable of detection in the physiological range are critical for an effective sensor. A POC device, utilizing multimarker detection, will be crucial for monitoring fertility levels. For multimarker detection, the shift in frequency for each hormone will reduce signal overlap.[34] Such overlap prevents the need for deconvolution, a method of reducing overlap or noise through signal resolution.[35] Therefore, the complexity of detecting each hormone will be reduced in the new biosensor.

C. Nontarget Interference

1. Purpose and Experimental Results

The purpose of nontarget testing is to verify the specificity of the antibody immobilized on the surface of the GDE. We sought to verify that anti-FSH was specific to FSH, without significant response from nontarget molecules. From a comparison of the imaginary impedance of each biomarker at the OBF of FSH (Fig. 6), greater sensitivity to FSH was observed. Estradiol, progesterone, and albumin impedance remained at similar values as concentration increased.

Further analysis of the logarithmic slope of each biomarker (Fig. 7) found the slopes of FSH, estradiol, albumin, and progesterone to be −28.08, −3.978, −10.89, and −10.27 Ohm/[Ln(pg/mL)], respectively. The slopes indicate a strong response to FSH, 7.06 times the response of estradiol, and 2.58

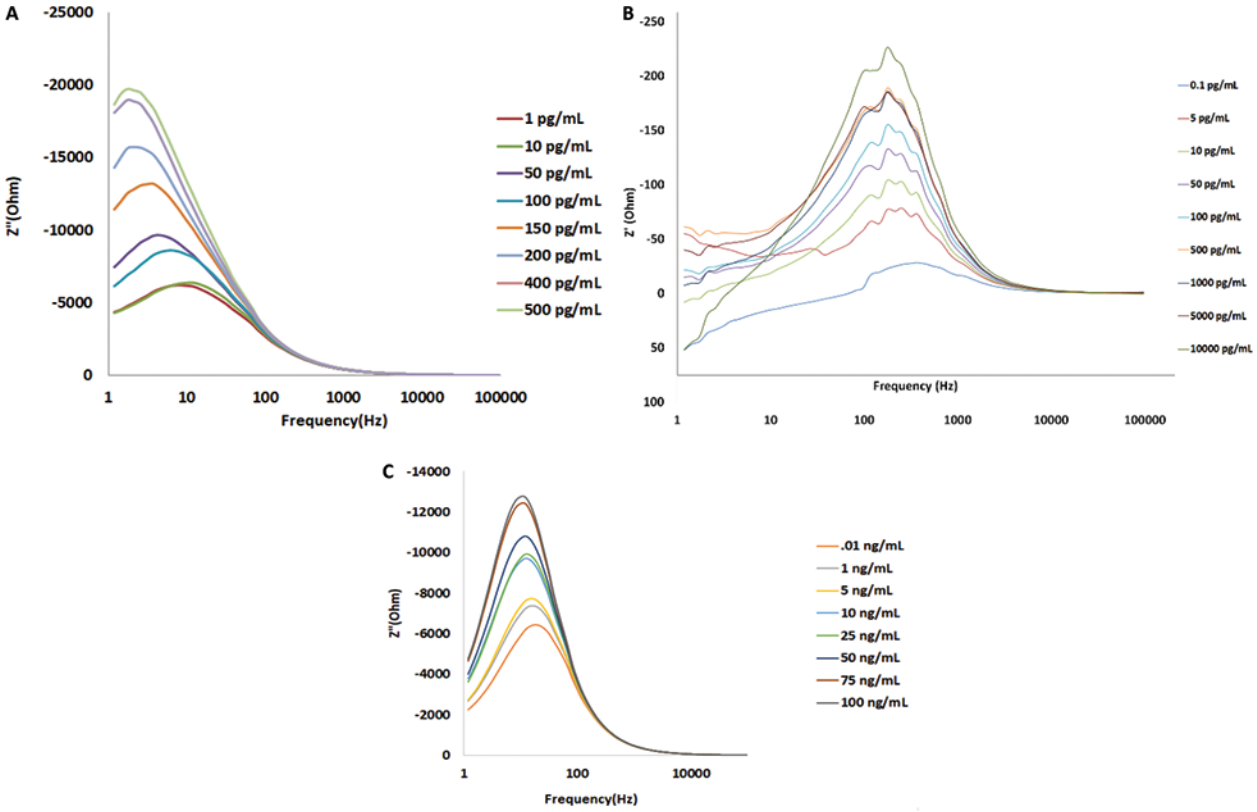

FIG. 3: (A) Overlay generated from the averaged imaginary impedance of N = 3 repetitions of all FSH concentrations from 0.1 to 10,000 pg/mL across frequencies ranging from 1 to 100,000 Hz. As expected, the imaginary impedance increases with concentration, and signal is lost at both extremes of the frequency spectrum. The blank response was subtracted from all data points to remove noise from the overlay. (B) Displays the overlay of average imaginary impedance readings across frequency for estradiol concentrations of 1, 10, 100, 200, 300, 400, and 500 pg/mL. Three repetitions were performed for each concentration. (C) The figure shows overlays of average imaginary impedance across frequency with three repetitions for each progesterone concentration of .01, 1, 5, 10, 25, 50, 75, and 100 ng/mL.

and 2.73 times the response of albumin and progesterone, respectively. These results were somewhat expected, with a negligible response to estradiol, and a significantly diminished, but nonnegligible response to progesterone and albumin. Estradiol was the sole hormone to exhibit extremely reduced response, which indicates that FSH may share some similarities with albumin and progesterone that is not shared with estradiol. Notably, the imaginary impedance response of albumin began experiencing large increases at 3,400 mg/dL, with a slope of only −2.793 Ohm/[Ln(pg/mL)]. In the analysis presented above, it is desirable to observe a very large slope response for FSH and far smaller slopes for all other biomarkers. Such differences in slope indicate either a lack of significant chemical interaction between the nontargets and anti-FSH, or very high specificity with FSH.

2. Detection in Blood

A crucial component of the proposed sensor is its ability to detect the target hormone in blood, which would be the preferred testing medium. To determine the antibodies effectiveness in blood, anti-FSH was immobilized and concentration gradients of FSH spiked whole-blood concentrations (1%–90%) were run in AC impedance mode. White New Zealand female rabbit whole blood from Bioreclamation was used, as detailed in the Mate-

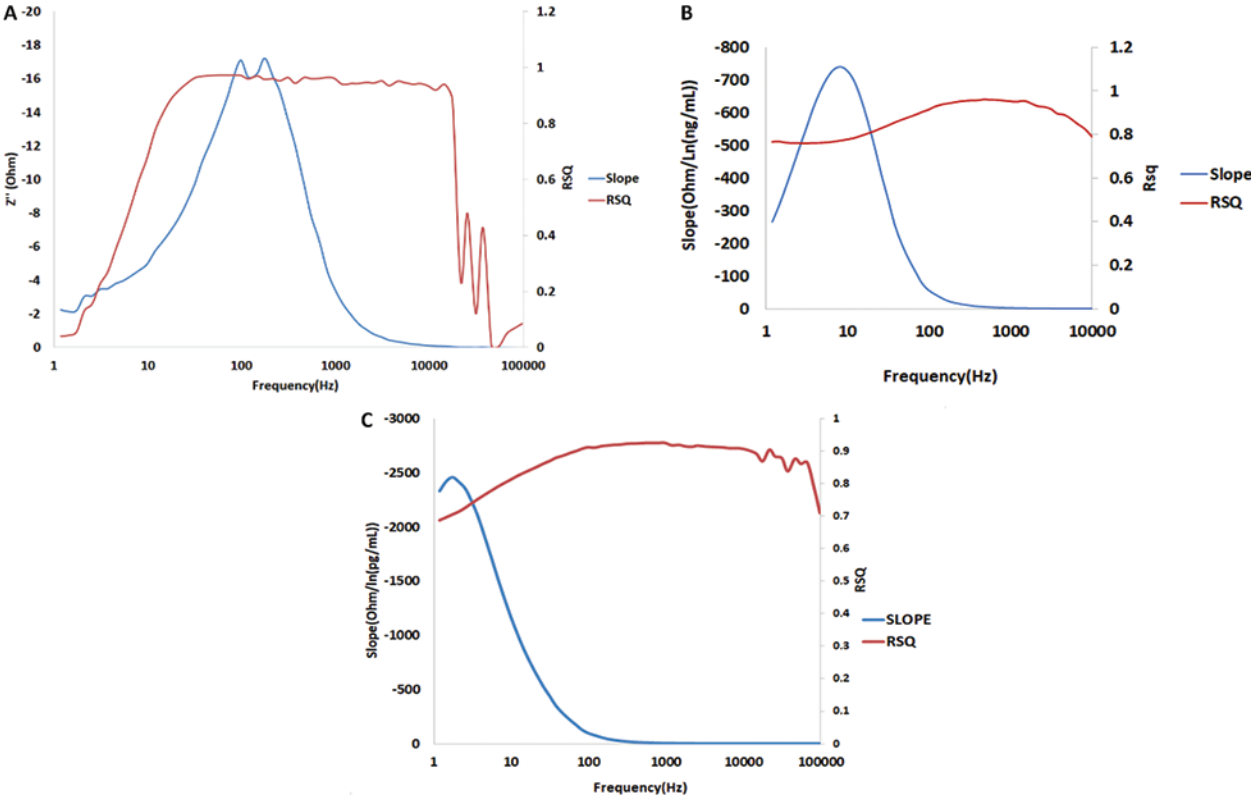

FIG. 4: (A) Shows the comparison of logarithmic slope and R^2 calculated from FSH imaginary impedance across all chosen frequencies. By calculating the frequency at which the slope is maximized, the OBF of FSH can be found at 175.8 Hz. (B) A representation of logarithmic slope and R^2, fitting average imaginary impedance values for progesterone concentrations across the frequency sweep. The optimal binding frequency was determined to be 8.071 Hz. (C) Displays the fit for average imaginary impedance readings for target estradiol concentrations across the frequency sweep, with logarithmic slope and RSQ. Optimal binding frequency was 1.74 Hz.

rials and Methods section. The resulting slope and R^2 values of the calibration curves created at FSH's OBF (175.8 Hz) were calculated to visualize where the sensor is still effective and where it fails without any filtering methods. A similar process was used for estradiol using 5%, 10%, and 90% dilutions. The slope of each hormone at the corresponding blood dilutions were graphed alongside the calibration curves of each hormone in 90% blood and in PBS solution (Fig. 8). Although the 10% blood dilution produced the highest average response across both hormones, the 90% blood dilution data was analyzed because it more closely represents whole blood. The slope response of FSH decreased greatly as blood concentration increased up to 25% blood, where the slope remained level at approximately −15 Ohm/[Ln(pg/mL)], likely due to increasing interference with anti-FSH binding. Although slopes may have stabilized for blood percentages, there could have been background levels of FSH that caused changes in slope. Figure 8 displays a concentration of 0 pg/mL for FSH within the 90% blood sample. It could be offset if the concentration of FSH could be > 1 pg/mL.

Estradiol exhibited entirely different results, with very large slopes at both 10% and 90% blood. The following findings suggest that antiestradiol undergoes very little interference from blood compared to FSH, possibly due to difference in molecular weight (i.e., FSH is 36 KDa while estradiol is only 0.272 KDa). As shown in the calibration curves in Fig. 8, the 90% blood solutions exhibit

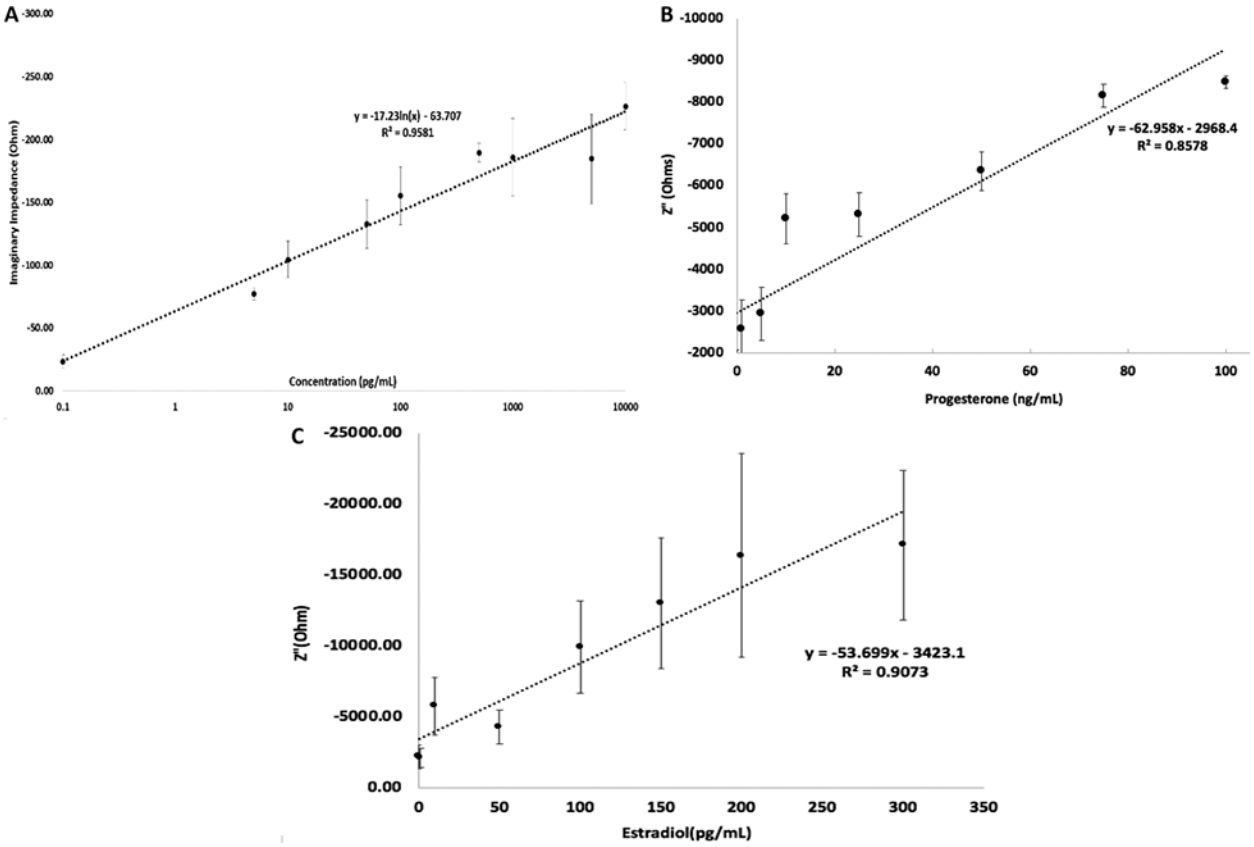

FIG. 5: (A) Calibration curve of imaginary impedance values over FSH concentrations of 0.1, 5, 10, 50, 100, 500, 1,000, 5,000, and 10,000 pg/mL at 175.8 Hz, the OBF for FSH. The trendline y = −17.23ln(x) −63.707 confirms a linear relationship between imaginary impedance and concentration. A high R^2 value of 0.9581 shows the data to be highly reproducible, with errors calculated as standard error with n = 3. (B) Calibration curve of 01, 1, 5, 10, 25, 50, 75, and 100 ng/mL derived from average imaginary impedance values for progesterone concentrations at optimal binding frequency of 8.071 Hz. A linear relationship is confirmed with the trendline (y = −62.958x −2968.4) and the reproducibility of the data is confirmed through the RSQ value of .8578. (C) Representation of a calibration curve for estradiol concentrations of 1, 10, 100, 200, 300, 400, and 500 pg/mL, determined through average imaginary impedance values with N = 3 repetitions. The curve is based off the optimal binding frequency of 1.74 Hz. The trendline (y = −53.699x −3423.1) and the RSQ value of .9073 confirm the linear relationship and the reproducibility of the data, respectively.

higher overall impedance, which is expected for solutions with additional particulate matter. However, with only one trial, the RSQs are quite low at only 0.1511 for FSH and 0.291 for progesterone. Thus, although anti-estradiol is likely capable of selectively binding estradiol in blood, the immobilized anti-FSH sensor on its own was not selective enough in blood. A finalized device will need to include a filtration method to eliminate some of the larger proteins and other possible contaminants prior to being exposed to the antibody. A Nafion coating on the electrode is a potential solution; it would provide protection from anionic interferents with a simple mode of incorporation into the sensor platform.[36]

Our nontarget analysis of anti-17 β-estradiol confirmed that the antibody is selective, even in physiological levels of albumin (a large protein found in blood). Therefore, future work will focus on determining which features of blood cause the

TABLE 1: A summary of the responses each target hormone and antibody have in when paired in a pure system of redox probe and phosphate buffered saline

Target	n	Optimal Binding Frequency (Hz)	Slope	R^2	Lower limit of detection	Physiological Range
Progesterone	3	8.071	−62.958	0.86	8.22 ng/mL	1–30 ng/mL
Estradiol	3	1.74	−53.699	0.8	2.35 pg/mL	1–500 pg/mL
FSH (Follicle Stimulating Hormone)	3	175.8	−17.23	0.91	4.02 pg/mL	100–6000 pg/mL

decreased signal and on trying to block these specific contaminants.

3. Implications and Future Work

Figure 5 clearly shows each biomarker that measures across a specific and narrow range of imaginary impedance values. This result was expected because the characteristics of each molecule uniquely affect the impedance. Only FSH shows a consistent relationship between concentration and imaginary impedance. Our observations indicate that the anti-FSH antibody is far more responsive to variations in FSH concentration than the nontarget hormones tested. Thus, when carried out at its OBF, FSH can selectively bind to anti-FSH. Other antibodies are far less capable of binding to their target hormone at the frequency. The implication that anti-FSH can bind selectively with FSH at its OBF is critically important for the future development of a multimarker sensor for fertility. As other key fertility hormones displayed reduced chemical activity at frequencies distant from their OBF, antibodies could potentially be immobilized onto a sensor surface with another antibody and exposed to solutions containing more than one hormone without

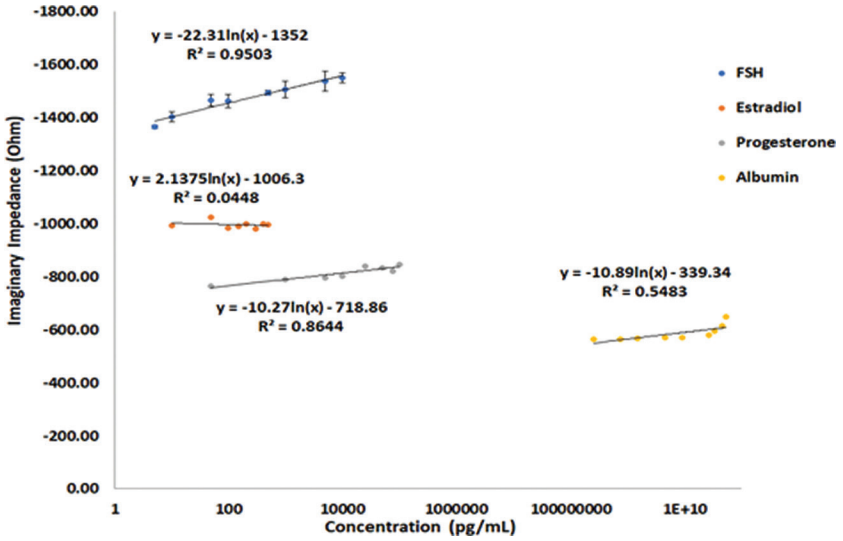

FIG. 6: Scatterplot showing imaginary impedance of the target molecule (FSH), and interferent molecules of estradiol, progesterone, and albumin at the optimal binding frequency of FSH (175.8 Hz). Concentrations were determined based upon the physiological range of each molecule. FSH ranged between 0.1 and 10,000 pg/mL; estradiol ranged between 10 and 500 pg/mL; progesterone ranged between 0.05 and 100 ng/mL; and albumin ranged between 25 and 5,400 mg/dL.

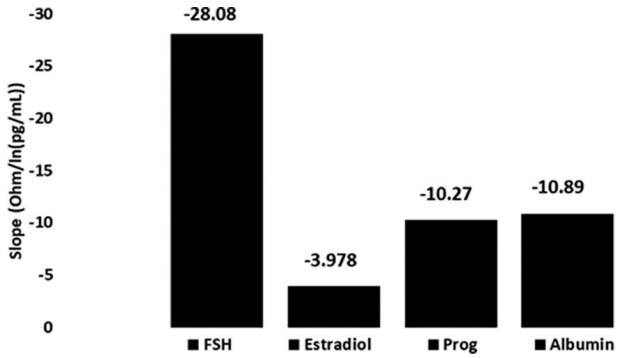

FIG. 7: The logarithmic slope of each molecule in the scatter plot from Fig. 6. The slope of FSH was −28.08, and the slopes of estradiol, progesterone, and albumin were −3.978, −10.27, and −10.89, respectively. Because the analysis was performed at its optimal binding frequency, the slope of FSH was significantly higher than the slope of any other molecule. Each biomarker concentration was chosen based upon its physiological range: FSH was calculated between 5 and 10,000 pg/mL, estradiol between 10 and 500 pg/mL, progesterone between 0.05 and 100 ng/mL, and albumin

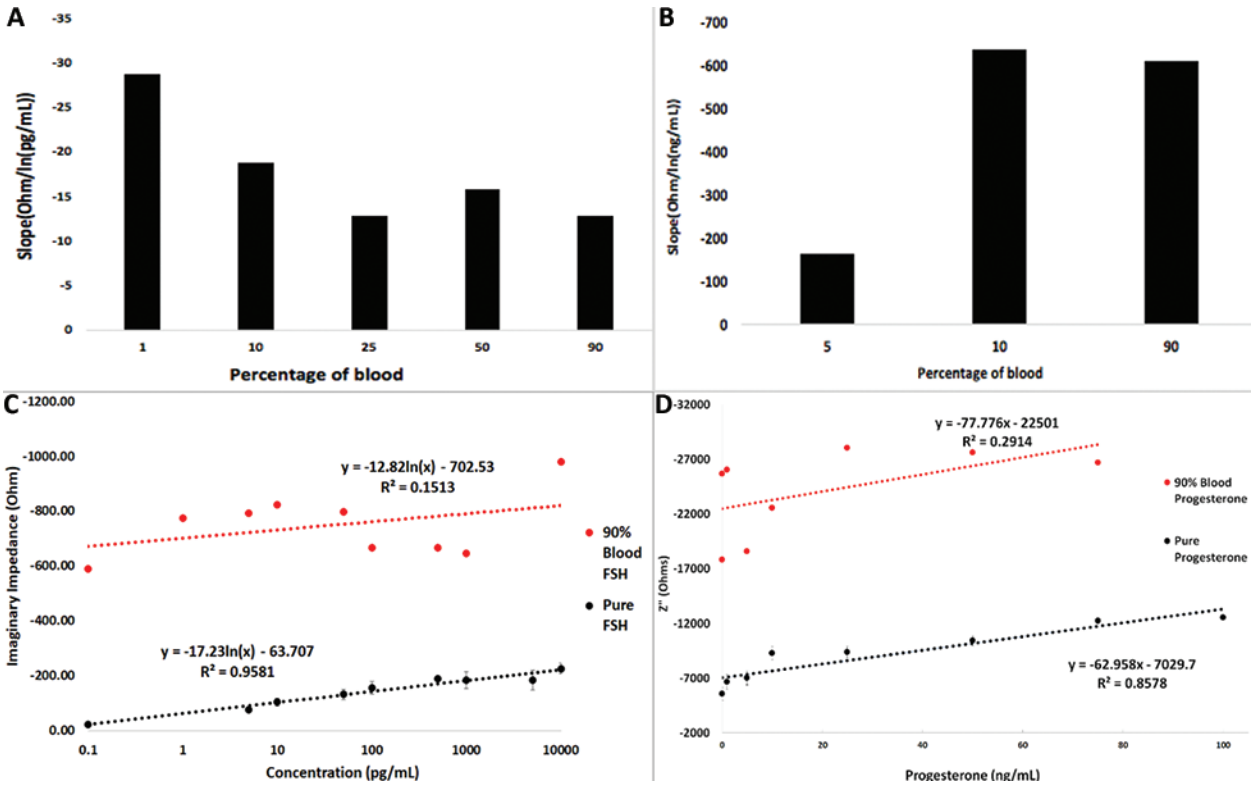

FIG. 8: (A) Comparison of FSH logarithmic slope at various percentages of blood mixed with phosphate buffered saline (PBS) from 1% to 90%. Slope was calculated from the imaginary impedance of FSH at each % blood; it displays an initial decrease with increasing blood concentrations, but little change is apparent between the higher concentrations. (B) Comparison of progesterone logarithmic slope at various % blood mixed with PBS at 5%, 10%, and 90%. The slope shows a dramatic increase between 5% and 10%, but little change between 10% and 90%. (C) Calibration curves of pure FSH in solution and of 90% blood solution, both with added FSH between 1 and 10,000 pg/mL. (D) Calibration curves of pure progesterone in solution and 90% blood solution, with added estradiol between 0.1 and 100 pg/mL.

significant interference. In future studies utilizing solutions with multiple hormones, we expect that FSH will bind selectively with the antibody with negligible interference from other chemicals or hormones. As a result, we believe that the concentration of FSH can be accurately determined, even in complex solutions such as blood.

IV. CONCLUSIONS

The ability to determine peak levels of ovulation during normal menstrual cycles from concentrations of estradiol, FSH, and progesterone is a novel approach to the development of biosensors for testing fertility. Electrochemical detection offers the potential for detecting ovulation peaks, enabling fertility to be tested and tracked with greater accuracy and convenience for users by using blood samples. We believe that measuring devices similar to those used for blood glucose monitoring can be developed.

In the study, β-estradiol, FSH, and progesterone were characterized for the purpose of developing a multimarker fertility sensor. Using gold disk electrodes and electrochemical impedance spectroscopy, the optimal binding frequency of each hormone was determined. At these frequencies, a strong and reproducible linear relationship between log concentration and imaginary impedance (Z″/ohm) was established. An antibody specificity analysis was also completed with anti-FSH and nontargets to prove that FSH was the only hormone detected by anti-FSH. Results confirmed the specificity of FSH to its antibody. All nontarget molecules had slopes below −10.89 Ohm/[Ln(pg/mL)] at the FSH OBF. Conversely, FSH had a slope of −28.08 Ohm/[Ln(pg/mL)] at the OBF.

Finally, to show proof of concept, blood analysis was performed to determine how an antibody (anti-FSH) would select for its target (FSH). The analysis was performed under conditions the finalized sensor would experience. Although 1% blood dilution resulted in selective detection for the target, 90% blood dilution illustrated that a different method for the final device would be required. For instance, Nafion coating can be implemented to avoid potential contaminants and blood interferents. Our future work will include simultaneous detection of all three target hormones. To create a multimarker sensor, each molecular recognition element must be immobilized onto the same surface so all target concentrations can be calculated. The electrochemical characterization of these three hormones could lead one to develop a device to test the level of fertility hormones using electrochemical impedance spectroscopy, with the creation of a specific profile for each target.

REFERENCES

1. Cedars M, Jaffe RB. Infertility and women. J Clin Endocrinol Metab. 2005 Apr 1;90(4):E2.
2. Chandra A, Copen C, Stephen E. Infertility service use in the United States: data from the National Survey of Family Growth, 1982–2010, No. 73. National Center for Health Statistics: Atlanta, GA; 2014:1–21.
3. Krysiewicz S. Infertility in women: diagnostic evaluation with hysterosalpingography and other imaging techniques. Am J Roentgenol. 1992;159(2):253–61.
4. Martyn F, McAuliffe FM, Wingfield M. The role of the cervix in fertility: is it time for a reappraisal? Human Reprod. 2014 Oct 10;29(10):2092–98.
5. Lyons RA, Saridogan E, Djahanbakhch O. The reproductive significance of human fallopian tube cilia. Human Reprod Update. 2006 Aug 1;12(4):363–72.
6. Opsahl MS, Miller B, Klein TA. The predictive value of hysterosalpingography for tubal and peritoneal infertility factors. Fertil Steril. 1993 Sep 1;60(3):444–48.
7. Practice Committee of the American Society for Reproductive Medicine. Aging and infertility in women. Fertility and Sterility. 2006;86(5):S248–52.
8. Kumar TR, Wang Y, Lu N, Matzuk MM. Follicle stimulating hormone is required for ovarian follicle maturation but not male fertility. Nat Genet. 1997;15(2):201–4.
9. Raju GAR, Chavan R, Deenadayal M, Gunasheela D, Gutgutia R, Haripriya G, Govindarajan M, Patel NH, Patki KS. Luteinizing hormone and follicle stimulating hormone synergy: a review of role in controlled ovarian hyper-stimulation. J Human Reprod Sci. 2013;6(4):227–34.
10. Chappel SC, Howles C. Review: Reevaluation of the roles of luteinizing hormone and follicle-stimulating hormone in the ovulatory process. Hum Reprod. 1991 Oct 1; 6(9):1206–12.
11. Barnhart K, Osheroff J. Follicle stimulating hormone as a predictor of fertility. Curr Opin Obstet Gynecol 1998; 10(3):227–32.
12. De Placido G, Alviggi C, Mollo A, Strina I, Varricchio MT, Molis M. Recombinant follicle stimulating hormone is effective in poor responders to highly purified follicle stimulating hormone. Human Reprod. 2000 Jan 1;15(1):17–20.
13. Jirge PR. Poor ovarian reserve. J Human Reprod Sci. 2016;9(2):63–69.

14. Kumar P, Sait SF. Luteinizing hormone and its dilemma in ovulation induction. J Human Reprod Sci. 2011;4(1):2–7.
15. Lévy DP, Navarro JM, Schattman GL, Davis OK, Rosenwaks Z. The role of LH in ovarian stimulation. Exogenous LH: let's design the future. Human Reprod. 2000 Nov 1;15(11):2258–65.
16. Young KA, Chaffin CL, Molskness TA, Stouffer RL. Controlled ovulation of the dominant follicle: a critical role for LH in the late follicular phase of the menstrual cycle. Human Reprod. 2003 Nov 1;18(11):2257–63.
17. Young S, Lessey B. Progesterone function in human endometrium: clinical perspectives. Semin Reprod Med. 2010;28(01):5–16.
18. Shah D, Nagarajan N. Luteal insufficiency in first trimester. Indian J Endocrinol Metab. 2013;17(1):44–49.
19. Reed BG, Carr BR. The Normal Menstrual Cycle and the Control of Ovulation. In: Feingold KR, Anawalt B, Boyce A, Chrousos G, Dungan K, Grossman A, et al., editors. Endotext [Internet]. South Dartmouth (MA): MDText.com, Inc.; 2000 [cited 2019 Mar 19]. Available from: http://www.ncbi.nlm.nih.gov/books/NBK279054/.
20. Stricker R, Eberhart R, Chevailler M-C, Quinn F, Bischof P, Stricker R. Establishment of detailed reference values for luteinizing hormone, follicle stimulating hormone, estradiol, and progesterone during different phases of the menstrual cycle on the Abbott ARCHITECT® analyzer. Clin Chem Lab Med. 2006;44(7):883–7.
21. Panchal S, Nagori C. Imaging techniques for assessment of tubal status. J Human Reprod Sci. 2014;7(1):2–12.
22. Honikel M, Lin C, Probst D, La Belle J. Facilitating earlier diagnosis of cardiovascular disease through point-of-care biosensors: a review. Crit Rev Bio Eng. 2018;46(1):53–82.
23. Bidwell SE, Buck AA, Diesfeld HJ, Enders B, Huldt G, Kent NH, Kirsten C, Mattern P, Ruitenberg EJ, Voller A. The enzyme-linked immunosorbent assay (ELISA). Bull World Health Org. 1976;54(2):129–39.
24. Behre HM, Kuhlage J, Gaβner C, Sonntag B, Schem C, Schneider HP, Nieschlag E. Prediction of ovulation by urinary hormone measurements with the home use ClearPlan® Fertility Monitor: comparison with transvaginal ultrasound scans and serum hormone measurements. Human Reprod. 2000 Dec 1;15(12):2478–82.
25. Tanabe K, Susumu N, Hand K, Nishii K, Ishikawa I, Nozawa S. Prediction of the potentially fertile period by urinary hormone measurements using a new home-use monitor: comparison with laboratory hormone analyses. Human Reprod. 2001 Aug 1;16(8):1619–24.
26. Star A, Tu E, Niemann J, Gabriel J-CP, Joiner CS, Valcke C. Label-free detection of DNA hybridization using carbon nanotube network field-effect transistors. Proc Natl Acad Sci U S A. 2006 Jan 24;103(4):921.
27. Bhavsar K, Fairchild A, Alonas E, Bishop DK, La Belle JT, Sweeney J, Alford TL, Wang J, Bhavanandan VP, Joshi L. A cytokine immunosensor for multiple sclerosis detection based upon label-free electrochemical impedance spectroscopy using electroplated printed circuit board electrodes. Biosensor Bioelectron. 2009 Oct 15;25(2):506–9.
28. Adamson TL, Cook CB, La Belle JT. Detection of 1,5-anhydroglucitol by electrochemical impedance spectroscopy. J Diabetes Sci Technol. 2014 Mar;8(2): 350–55.
29. Honikel MM, Lin C-E, Cardinell BA, La Belle JT, Penman AD. Direct measurement of a biomarker's native optimal frequency with physical adsorption based immobilization. ACS Sens. 2018 Apr 27;3(4):823–31.
30. Fairchild A, McAferty K, Demirok UK, La Belle J. A label-free, rapid multimarker protein impedance-based immunosensor. 2009 ICME International Conference on Complex Medical Engineering; 2009 April 9–11; Tempe, AZ. New Jersey: IEEE Xplore Digital Library.
31. Py-Daniel KR, Pires Junior OR, Cordova CMI, Fascineli ML, Tedesco AC, Azevedo RB. HPLC-FLD method for itraconazole quantification in poly lactic-co-glycolic acid nanoparticles, plasma and tissue. J Brazil Chem Soc. 2014;25:697–703.
32. Lin C, Malkoc A, Probst D, Khanwalker M, Beck C, B Cook C, La Belle J. Enhancing glycemic control via detection of insulin using electrochemical impedance spectroscopy. J Diabetes Sci Technol. 2017;11(5):930–5.
33. Maheshwari A, Fowler P, Bhattacharya S. Assessment of ovarian reserve—should we perform tests of ovarian reserve routinely? Human Reprod. 2006 Nov 1;21(11): 2729–35.
34. Korcan Demirok U, Verma A, La Belle J. The development of a label-free electrochemical impedance based point-of-care technology for multimarker detection. J Biosens Bioelectron. 2013;Mar 20;S(12):1–7.
35. Stefan W, Garnero E, Renaut RA. Signal restoration through deconvolution applied to deep mantle seismic probes. Geophys J Int. 2006 Dec 1;167(3):1353–62.
36. Vaidya R, Atanasov P, Wilkins E. Effect of interference on the performance of glucose enzyme electrodes using Nafion® coatings. Med Eng Phys. 1995 Sep 1;17(6):416–24.